RESEARCH ARTICLE

Phenalenone-photodynamic therapy induces apoptosis on human tumor cells mediated by caspase-8 and p38-MAPK activation†

Abbreviated title: *PN-PDT induces apoptosis on tumor cells*

María L. Salmerón[1], José Quintana-Aguiar[2], Juan V. De La Rosa[3], Félix López-Blanco[3], Antonio Castrillo[3], Germán Gallardo[3] and Carlos Tabraue[3,4]*

[1]Departamento de Ciencias y Recursos Naturales, Facultad de Ciencias, Universidad de Magallanes, Punta Arenas, Chile.
[2]Departamento de Bioquímica y Biología Molecular, Fisiología, Genética e Inmunología. Instituto Universitario de Investigaciones Biomédicas y Sanitarias (IUIBS), Universidad de Las Palmas de Gran Canaria, Spain.
[3]Unidad de Biomedicina Asociada al Consejo Superior de Investigaciones Científicas (Instituto de Investigaciones Biomédicas "Alberto Sols" CSIC-Universidad Autónoma de Madrid), Instituto Universitario de Investigaciones Biomédicas y Sanitarias (IUIBS), Grupo de Investigación Medio Ambiente y Salud (GIMAS), Universidad de las Palmas de Gran Canaria, Spain.
[4]Departamento de Morfología, Universidad de Las Palmas de Gran Canaria, Spain.

†This article has been accepted for publication and undergone full peer review but has not been through the copyediting, typesetting, pagination and proofreading process, which may lead to differences between this version and the Version of Record. Please cite this article as doi: [10.1002/mc.22875]

Received 18 February 2018; Revised 23 June 2018; Accepted 18 July 2018
Molecular Carcinogenesis

DOI 10.1002/mc.22875

* Corresponding Author:
Carlos Tabraue, Ph.D.
Unidad de Biomedicina Asociada al Consejo Superior de Investigaciones Científicas (CSIC), Instituto Universitario de Investigaciones Biomédicas y Sanitarias (IUIBS) and Departamento de Morfología, Universidad de Las Palmas de Gran Canaria.
C/ Blas Cabrera Felipe s/n
Las Palmas de Gran Canaria, 35016
Spain
Phone: 0034928459681
Email: carlos.tabraue@ulpgc.es

Grant support

This work was supported in part by the Universidad de Las Palmas de Gran Canaria [Grant ULPGC2009-14].

Abbreviations

PN, Phenalenone; PDT, photodynamic therapy; PS, photosensitizer; ROS, reactive oxygen species.

Abstract

Photodynamic therapy (PDT) is a rising and hopeful treatment for solid tumors and others malignancies. PDT uses harmless visible light to activate a tumor-associated photosensitizer (PS). The excited PS generates cytotoxic reactive oxygen species (ROS) that induce damage and death of tumor cells. It is known that certain phytoalexins and phytoanticipins derived from plants often display a PS-like activity due to a phenalenone (PN) moiety -an efficient singlet oxygen photosensitizer- in its skeleton. The aim of this study is to explore the phototoxic properties of PN on the human cell line tumor-derived HL60 (acute promyelocytic leukemia) and to identify the cell-specific targets of ROS involved in the tumor cell death. Our results reveal that PN acts as an excellent PS, showing a potent antitumor cell activity in presence of light. PN-PDT generates intracellular ROS, via oxidation reaction mechanisms type I and II, resulting in an induction of apoptosis. Moreover, both extrinsic (through direct activation of caspase-3) and intrinsic (through mitochondrial depolarization) pathways of apoptosis are induced by PN-PDT. Using pharmacologic inhibitors, we also find that PN-PDT activates caspase-8/tBid and p38-MAPK, triggering the activation of the apoptotic pathways. Although, survival pathways are also promoted through PI3K/Akt and JNK activation, the net result of PN-PDT is the tumor cell death. The present work identifies to PN, for the first time, as a potent photosensitizer in human tumor cell lines and proposes a mechanism by which ROS induces apoptosis of tumor cell.

Key words

Phenalenone

Photodynamic therapy

Tumor cell

Apoptosis

ROS

Introduction

Photodynamic therapy (PDT) is a promising and minimally invasive therapeutic modality for treatment of a variety of solid tumors and certain non-oncological diseases. The process involves uptake of a photosensitizer (PS) drug into target cells followed by localized light irradiation in the visible wavelength (400-750 nm). Neither of these components alone display cytotoxic effects but when they are combined, in presence of molecular oxygen, they generate reactive oxygen species (ROS) inducing tumor cells death [1]. The specific light delivery to tumor cells provides a better selectivity for the targeting of cancers compared to conventional chemo- and radiotherapy. This aspect is important in the cancer treatment because PDT allows eradicate the maximum number of malignant cell types without unacceptable adverse effects produced by other types of therapies [2]. A PS is a light-absorbing molecule that is activated by light of an appropriate wavelength. The excited PS is able to promote radicals oxidation reactions (type I mechanism) from cellular targets to generate various reactive oxygen derivatives such as hydroxyl radical ($HO^{\bullet}$), superoxide radical anion ($O_2^{\bullet -}$) or peroxyl radical ($ROO^{\bullet}$). The excited PS can also transfer its energy to molecular oxygen (type II mechanism) to form the highly oxidizer singlet oxygen ($^1O_2$) [3]. ROS generation causes an oxidative damage to a variety of subcellular targets, carrying inevitably to cell death and resulting in the ablation of the tumor [4]. In addition, other mechanisms have been shown to be involved in the anti-carcinogenic effects of PDT, as shutting down of the tumor vasculature, starving of oxygen or nutrients to the tumor and the induction of a host immune response [5,6].

PDT-induced cell death may occur by apoptosis, autophagy or necrosis, however apoptosis is the mechanism mainly activated [4,7,8]. Apoptosis is a physiological event, which can also be triggered by external stimuli such as oxidative stress attributable to photosensitization. The involvement of apoptosis as mechanism of cell death has been shown to be an early response of PDT, both *in vitro* as *in vivo* [9,10]. Two major apoptotic pathways have been characterized in PDT: the death receptor-mediated or extrinsic pathway and the mitochondria-mediated or intrinsic pathway. In the first pathway, cell surface receptors related with tumor necrosis factor (TNF) gene family are stimulated, activating the initiator caspase-8 via adaptor and scaffolding proteins. The second process is triggered by disruption of mitochondrial function, which causes release of cytochrome c. Cytosolic cytochrome c binds to Apaf-1 inducing Apaf-1 oligomerization in presence of dATP. This complex, termed apoptosome, recruits and activates the initiator caspase-9. In both pathways, the activation of initiator caspases (caspase-8 or caspase-9) leads to the activation of effector caspases (caspase-3, -6 and -7) and cell death by apoptosis [4,11]. In addition, other signalling molecules involved in stress or survival pathways may be activated in PDT [12,13]. In fact, modulating of this signalling molecules can increase photokilling of cancer cells with defects in apoptotic pathways, which is a crucial step in carcinogenesis and therapy resistance [14].

Since the hematoporphyrin derivative Photofrin® was approved in 1993 as a PDT-sensitizer for treating bladder cancer, the development of new PS have improved PDT efficacy [15]. Second-generation PSs for clinical treatment include porphyrin and non-porphyrin derivatives. Porphyrin derivatives as 5-aminolevulinic acid (ALA), chlorins (benzoporphyrins), phthalocyanines, texaphyrins, pheophorbides (derived from chlorophyll) and bacteriopheophorbides (derived from bacteriochlorophyll) are being used for PDT of a great variety of solid tumors or it have been approved for use in clinical trials for different types of cancer. Non-porphyrin derivatives as anthraquinones (hypericin), phenothiazines (methylene blue), xanthenes (rose bengal), cyanines and curcuminoids are being evaluated in clinical trials for treatment of different types of cancer, or are used for treatment of no-oncological diseases. In addition, some of non-porphyrin PS are used in other fields of the medicine due to their antibacterial, antiviral and antimicrobial activities, or staining properties on tumor tissues [16]. Currently, new or derivatives PSs with improved spectroscopic, photochemical and tumor-localizing properties are being tested, expanding the scope of the PDT in the treatment against cancer.

Phenalenone or 1-H-phenalen-1-one (Fig.1A), also known as perinaphthenone (PN), is an efficient $^1O_2$ PS, which is distinguished by a quantum yield close to unity in solvents of very different polarity [17,18]. This tricyclic aromatic ketone is a unique class of bioactive natural products with diverse structural features and widely distributed in the nature. In the last years, numerous and new classes of natural products based on the PN skeleton has been isolated from plants and fungi or has been chemically synthesized. These molecules are of special interest owing to their significant roles as phytoalexins and phytoanticipins in the protection of plants against potentially harmful microorganisms such as fungus [19–22] and protozoans [23,24]. In addition, these compounds display ROS-mediated activity against disease vector mosquito larvae and plant-parasitic nematodes, which is strongly enhanced in the presence of light [25,26]. This phenomenon is in accordance with the presence of PN in the skeleton of these molecules. In addition, PN derivatives have also been developed as dental drugs for photodynamic inactivation of oral key bacteria [27]. These previous data led us to investigate the photobiological properties of phenanelone, since novel molecules or natural compounds derived from plants, based on PN moiety, might be used as potential PS agents in PDT for cancer treatments.

Here, using human promyelocytic leukemia cells HL60 as tumor cell model we prove that PN-PDT exerts a strong phototoxic action as consequence of a ROS-mediated apoptosis. We also found that ROS generated during PN-PDT activate caspase-8, driving the apoptotic signal through both extrinsic (activating directly caspase-3) and intrinsic (through tBid activation and mitochondrial depolarization) pathways. Besides, we demonstrate that ROS generation by PN-PDT activate the stress pathways p38MAPK and JNK, and promote the survival pathway PI3K/Akt. Interestingly, p38MAPK and JNK play opposing effects on cell survival. Blocking the activation of these kinases after PN-PDT with suitable inhibitors showed that the p38MAPK play

a role as a death signal, whereas the JNK serves as a rescue signal. Although survival pathways are activated, the net result of PN-PDT is a potent oxidative burst that finalizes irremediably with the apoptotic death of the tumor cell.

Materials and methods

Chemicals

All chemicals were of reagent grade and used as received. PN was purchased from Sigma Chemical Co. (St. Louis, MO), dissolved in dimetilsulfóxido (DMSO) and stored at -20 ºC. Cell culture media, animal serum, supplements and disposable cell culture equipment were purchased from Thermo Scientific (Grand Island, NY). Ascorbic acid, sodium azide, bis-benzimide trihydrochloride (Hoechst 33258), propidium iodide, 3-(4,5-Dimethylthiazol-2-yl)-2,5-diphenyltetrazolium bromide (MTT), labelled substrates for caspase-3 (Ac-DEVD-pNA), caspase-9 (Ac-LEHD-pNA) and caspase-8 (Ac-IETD-pNA), permeable inhibitors for caspase-3 (z-DEVD-fmk), caspase-9 (LEHD-CHO), caspase-8 (z-IETD-fmk), P38-MAPK (SB203580), JNK (SP600125), MEK1 (PD98059) and PI3K (LY294002) were from Sigma Chemical. Carbonyl cyanide m-chlorophenylhydrazone (CCCP) and fluorescent probes 2′,7′-dichlorodihydrofluorescein diacetate (H_2-DCF-DA) and 5,5',6,6'-tetrachloro-1,1',3,3'-tetraethylbenzimidazolylcarbocyanine iodide (JC-1) were purchased from Thermo Scientific. Antibodies against human p38-MAPK, phospho-p38-MAPK, JNK, Akt, phospho-Akt (Ser 473) and horseradish peroxidase-conjugated IgG secondary antibodies were from Cell Signalling Technologies (Danvers, MA). Antibodies against phospho-JNK, cytochrome c and COX IV were from abCAM (Cambridge, UK), caspase-8 from Enzo Life Sciences, Inc. (Farmingdale, NY) and Bid from BD Biosciences (Franklin Lakes (NJ). Pierce Chemical Co. (Rockford, IL) supplied reagents for the SuperSignal West Pico chemiluminescence detection of proteins on immunoblots.

Cell culture

HL-60 cells were cultured in RPMI 1640 medium supplemented with 10% (v/v) heat-inactivated fetal bovine serum (FBS), 100 U/mL penicillin and 100 µg/mL streptomycin at 37°C in a humidified atmosphere containing 5% CO_2. A431 and A549 cells were grown in Dulbecco's modified Eagle's medium (DMEM) supplemented with 10% fetal bovine serum, 100 units/ml penicillin and 100 µg/ml. These cell lines were obtained from the American Type Culture Collection (LGC Standards, Barcelona, Spain). The cultures exhibited characteristic doubling times of approximately 24 h and the growth medium was changed on the day before the experiment.

Photodinamic treatments

The cells were seeded out in 96-well or 10-cm plates and treated with different concentrations of PN at 37 ºC for 30 min, before light exposure from a CAMAG Reprostar II.

The irradiance of the lamps was set at 2.77, 8.33 or 11.15 mW cm^{-2} and was measured using a luxmeter Mavolux (Gossen, Nürnberg, Germany). The fluence or light dose delivered to the cells (5, 15 and 20 J cm^{-2}) was determined from the product of the irradiance and the duration of irradiation. After light exposure, cells were washed with PBS and incubated at 37 ºC in growth medium for the specified time in each experiment. In the experiments where inhibitors were tested the cells were pre-incubated with the specified inhibitor for 1 h and then treated with PN for 30 min before irradiation. In this case, the cells were washed with PBS and incubated with fresh growth medium containing the inhibitors.

Cell viability assay

Cells were seeded in 96-well plates at a density of 10^4 cells per well and the metabolic activity of the cells was determined on the basis of their ability to metabolize 3-(4,5-dimethylthiazol-2yl)-2,5-diphenyltetrazolium bromide (MTT) into formazan crystals. After treatments, the plates were centrifuged (1000 g, 10 min at room temperature) and the cells were incubated with 100 µL of MTT solution (0.5 mg/mL in RPMI medium) at 37 ºC for 4 h. The reaction was stopped with 100 µL of lysis buffer [20% sodium dodecyl sulfate (SDS) in 20 mM HCl] and formazan crystals were dissolved by incubation at 37 ºC overnight. Optical density was measured in a microplate reader Ceres 900C (Bio-Tek Instruments, Winooski, UT, USA) at 570 nm and results were expressed as percentage of cell viability relative to the untreated control. Three independent experiments were carried out in quadruplicates.

Quantitative fluorescent microscopy

Cells (~$5x10^5$) were collected, washed twice with PBS, and incubated with 75 µl 3% (w/v) paraformaldehyde at room temperature for 10 min. The fixative was removed and the cells were resuspended in 15 µl of PBS containing 20 µg/ml bis-benzimide trihydrochloride and incubated at room temperature for 15 min. Aliquots of cell suspension were placed on glass slides and triplicate samples of 500 cells each were counted and scored for the incidence of apoptotic chromatin condensation using a Zeiss fluorescent microscopy. Nuclei with condensed chromatin (supercondensed chromatin at the nuclear periphery) or nuclei that were fragmented into multiple smaller dense bodies were considered as apoptotic. Nuclei with uncondensed and dispersed chromatin were considered as non-apoptotic.

Detection of ROS generation

Intracellular ROS were determined by flow cytometry using H_2-DCF-DA, which is deacetylated by intracellular esterases and oxidized by peroxides into the fluorogenic probe DCF. After treatment, cells were further incubated for 30 min with H_2-DCF-DA (8 µM), washed twice with PBS, resuspended in 1 ml PBS and analyzed using a Coulter EPICS XL-MCL cytometer (Beckman-Coulter, Fullerton, CA, USA) with an excitation setting of 488 nm. The specific DCF-derived fluorescence was detected using a 525±20 nm band-pass filter. In each study, 10,000 cells were analyzed.

Assay of caspase activity

The cells were centrifuged at 500 g for 10 min at 4 ºC, washed twice with ice-cold PBS and lysed in caspase extraction buffer [50 mM HEPES (pH 7.4), 1 mM DTT, 0.1 mM EDTA, 0.1% Chaps] by pushing them several times through a 22-gauge needle. After centrifugation at 16,000 g for 10 minutes at 4 ºC the supernatants were analyzed for protein concentration by the bicinchoninic acid (BCA) dye-binding assay using bovine serum albumin (BSA) as a standard and aliquots containing ~20 µg of protein were evaluated for caspase activity. Labelled substrates for caspase-3, caspase-9 and caspase-8 activities were N-acetyl-Asp-Glu-Val-Asp-para-nitroaniline (Ac-DEVD-pNA), N-acetyl-Leu-Glu-His-Asp-para-nitroaniline (Ac-LEHD-pNA) and N-acetyl-Ile-Glu-Thr-Asp-para-nitroaniline (Ac-IETD-pNA), respectively. Caspase-catalyzed release of the chromophore para-nitroaniline (pNA) from the substrate was measured at 405 nm in a microplate reader Ceres 900C (Bio-Tek Instruments, Winooski, UT, USA) and specific activity was expressed as pmol pNA per minute and per microgram protein. Blanks containing the substrate alone were also included.

Quantification of apoptotic cells by flow cytometry

The cells were centrifuged at 500 g for 10 minutes at 4ºC, washed twice with 1 ml ice-cold PBS and resuspended in 50 µl PBS. Following drop-wise addition of 1 ml ice-cold 75% ethanol, fixed cells were stored at −20ºC for at least 1 hour. Samples were then centrifuged and washed as above. The cell pellets were resuspended with 1 ml PBS containing 50 µg/ml propidium iodide and 100 µg/ml RNase A, and incubated for 1 h at room temperature. The cell cycle phase distribution was analyzed by flow cytometry using a Coulter EPICS XL-MCL cytometer (Beckman-Coulter, Fullerton, CA, USA) with an excitation setting of 488 nm. The propidium iodide-derived fluorescence was detected using a 620±15 nm band-pass filter. A minimum of 10,000 cells per experimental condition was evaluated. Cell debris was excluded from analysis. The cells with reduced DNA staining (hypodiploid cells), resulting from either fragmentation or decreased chromatin, were considered apoptotic cells.

DNA fragmentation assay

The cells were washed twice with ice-cold PBS and incubated with 50 µL extraction buffer [10 mm Tris-HCl (pH 7.5), 1 mm EDTA, 0.2% Triton-X-100] for 15 min at 4 ºC. Cellular debris was removed by centrifugation (16,000 g for 10 min at 4 ºC) and the supernatants containing low molecular weight fragmented DNA were collected. Five microliters of RNase A (10 µg/µl) was then added and the mixture was incubated for 1 h at 37 ºC. The addition of 5 µl of proteinase K (10 µg/µl) was followed by an additional 1 h incubation at 37 ºC. DNA was extracted twice with 50 µL of phenol (pH 7.4) and once with 50 µl of phenol:chloroform:isoamilic alcohol (25:24:1). Aliquots of the aqueous phase (5-10 µl) was analyzed by electrophoresis on 2% agarose gel containing ethidium bromide (0.5 µg/µl) for 4 hr at 40 V in TAE buffer [40 mm

Tris-acetate (pH 8.0), 1 mm EDTA]. The gel was exposed to UV illumination and the image was captured (Digi-Doc, Bio-Rad Laboratories, Richmond, CA, USA).

Analysis of mitochondrial membrane potential ($\Delta\Psi_m$)

Cells were incubated with 10 μM of fluorescent probe 5,5',6,6'-tetrachloro-1,1',3,3'-tetraethylbenzimidazolylcarbocyanine iodide (JC-1) for the last 30 min of recovery, collected by centrifugation at 500 g for 10 min at room temperature and washed with PBS. JC-1 is a cationic dye that accumulates and aggregates into energized mitochondria (high $\Delta\Psi_m$) in healthy cells. After excitation JC-1 aggregates emit fluorescence at 590 nm. Upon cell injury, as mitochondrial membrane potential decreases, JC-1 aggregates are transformed back into JC-1 monomers, which emit fluorescence at 529 nm. Consequently, mitochondrial depolarization is indicated by a reduction in the red fluorescence. Cells were analyzed using a Coulter EPICS XL-MCL cytometer (Beckman-Coulter, Fullerton, CA, USA) with an excitation setting of 488 nm. Monomers- and aggregates-derived fluorescence were detected using 525±20 nm and 620±15 nm band-pass filters. A minimum of 10,000 cells per experimental condition was evaluated. Cell debris was excluded from analysis. Cells treated with 10 μM of the depolarizing agent carbonyl cyanide m-chlorophenylhydrazone (CCCP) for 30 min were used as a positive control; in these conditions >60% of cells exhibited low mitochondrial membrane potential.

Western blot analysis

The cells were centrifuged at 1,000 g for 10 min at 4 ºC and washed with ice-cold PBS. To obtain total cellular protein extracts, cell pellets were resuspended in lysis buffer [20 mM Tris-HCl (pH 7.4), 2 mM ethylenediaminetetraacetic acid (EDTA), 137 mM NaCl, 10% glycerol, 1% Triton X-100, 2 mM tetrasodium pyrophosphate, 20 mM sodium β-glycerophosphate, 10 mM sodium fluoride, 2 mM sodium orthovanadate] supplemented with protease inhibitors phenylmethylsulfonyl fluoride (PMSF, 1 mM), leupeptin (2 μg ml^{-1}), aprotinin (5 μg ml^{-1}) and pepstatin A (2 μg ml^{-1}). After incubation at 4 °C for 15 min, the lysates were sonicated on ice and centrifuged at 12,000 g for 10 min at 4°C and the soluble fraction (whole cell lysate) was stored at -70 ºC until used. To obtain subcellular fractions, cell pellets were resuspended in ice-cold isotonic buffer [20 mM HEPES (pH 7.5), 250 mM sucrose, 10 mM KCl, 1.5 mM $MgCl_2$, 1 mM EDTA, 1 mM ethylene glycol-bis(β-aminoethyl ether)-N,N,N',N'-tetraacetic acid (EGTA), 1 mM dithiothreitol (DTT)] supplemented with protease inhibitors as above. After 15 min incubation on ice, cells were lysed by pushing them several times through a 22-gauge needle and the lysates spun down at 1,000 g for 5 min at 4 °C to remove nuclei. The supernatant was centrifuged at 100,000 g for 15 min at 4 °C and the resulting supernatant (cytosolic fraction) and the precipitate (mitochondrial fraction) were stored at -70 ºC until used. Protein concentration was measured by the BCA method and samples containing equal amounts of proteins were boiled in SDS sample buffer and analyzed by SDS-polyacrylamide gel electrophoresis. Proteins were electrotransferred to PVDF membranes which were blocked with 5% fat-free dry milk in Tris-buffered saline [50 mM Tris-HCl (pH 7.4), 150 mM NaCl] with 0.1% Tween 20 and then incubated with specific antibodies against caspase-3, caspase-8, Bid, cytochrome c, COX-IV,

p38-MAPK, phospho-p38-MAPK, JNK, phospho-JNK, Akt and phospho-Akt for 24 h at 4°C. After washing and incubation with an appropriate horseradish peroxidase-conjugated secondary antibody, the antigen-antibody complexes were visualized by enhanced chemiluminescence.

Statistical analysis

Data are presented as mean ± SE. All determinations were performed in triplicate and the data shown are representative results from at least three independent experiments. Statistical differences between means were tested using (i) Student's t test (two samples) or (ii) one-way analysis of variance (ANOVA; three or more samples) with a posteriori pairwise comparisons of means carried out using Tukey's test. A significance level of $P<0.05$ was used.

Results

PN-PDT inhibits the cell viability of human tumor cell lines

Preliminary experiments were designed to determine whether PN presented phototoxic effects on human cancerous cells and to select the optimum conditions for PDT. For this purpose, we tested the photobiological activity of PN on the human tumor-derived cell lines HL60 (acute promyelocytic leukemia), A431 (epidermoid carcinoma) and A549 (lung adenocarcinoma). The cells were preincubated with increasing concentrations of PN for 30 min in darkness and then illuminated with broadband white light (11.15 mW cm^{-2}) for 30 min (fluence, 20 J cm^{-2}). Following a 24 h incubation period in fresh growth medium without PN, the effect of PDT on cell viability was analyzed using the MTT assay. As shown in Fig. 1B, in presence of white light PN showed concentration-dependent phototoxic properties in all cell lines evaluated, being HL-60 cells especially sensitive, with an IC_{50} as low as 5 μM. In contrast, in absence of white light, PN at the maximum concentration employed (30 μM) did not display toxicity on neither of cell lines. To confirm that the antiproliferative activity of PN was light-dependent, HL-60 cells were treated with PN and subjected to increasing doses of light or subjected to different exposure times to the light. The results clearly demonstrate that the reduction of cell viability in response to PN is dependent on the degree of fluence administrated to the cells (Fig. 1C) and on the exposure time to the light (Fig. 1D). The maximal effect was obtained with a fluence of 20 J cm^{-2} and 30 min of exposure to light. These results demonstrate that PN behave as an efficient PS since it decreases cell viability only in presence of light. Therefore, the following studies were performed on HL-60 cells as experimental model, using 5 μM PN for 30 min and subsequent illumination with broadband white light to a fluence of 20 J cm^{-2}.

PN induces apoptosis on human myeloid leukemia cells via intracellular ROS generation

In order to elucidate whether PN-PDT decreases cell viability through apoptosis activation, morphological changes characteristic of apoptotic cells were analyzed and quantified by fluorescent microscopy. As shown in Fig. 2A, the cells subjected to PN-PDT exhibited

condensed and fragmented chromatin (apoptotic bodies) in contrast to control cells treated with PN in absence of light that presented unfragmented and rounded nuclei. The quantification revealed that the percentage of apoptotic cells increased until 40,7% (8-fold) and 52,2% (10-fold) in PN-PDT treated cells, compared to control, after 6 h and 12 h of exposure, respectively (Fig. 2B). Consistent with these results PN-PDT caused DNA cleavage with the characteristic pattern of internucleosomal fragmentation, which is considered a hallmark of apoptosis (Fig. 2C). DNA fragmentation was detected at 2 h after photosensitization and increased progressively along the incubation time, whereas DNA from cells exposed to PN without irradiation remained unfragmented. Maximum levels of fragmented DNA were appreciated at 6 h of treatment. Apoptotic cells were also analyzed and quantified by flow cytometry after staining with propidium iodide (Fig. 2D and 2E). The results demonstrate that the percentage of hypodiploid cells (i.e. apoptotic cells) markedly raised from 2.6% to 25.6% (10-fold) in PDT-treated cells, compared to control, determined 2 h after exposure to light, and from 2.2% to 40.3% (20-fold) at 6 h post-exposure to light. Together, these results demonstrate that in presence of light PN is an inducer of cell death by apoptosis.

A recent study has described to PN as an effective PS, in organic solvents and in aqueous and lipid media, through the single electron transfer reactions [28]. To determine whether PN acts through generation of ROS in HL-60 cells, the levels of intracellular ROS were analyzed by flow cytometry. For this objective, the cells were incubated with the ROS-sensitive fluorescent probe H_2-DCF-DA during the last 30 min of PDT. This probe reacts with different intracellular ROS, mainly hydrogen peroxide (H_2O_2) and its radical derivatives, $HO^{\bullet}$ and peroxynitrites ($ROO^{\bullet}/NO^{\bullet}{}_2$) [29]. As shown in Fig. 3A and 3B, PN-PDT stimulates the generation of ROS in a concentration-dependent fashion of the PS (1-30 µM), suggesting that PN-induced apoptotic cell death could be mediated by the reactive oxygen derived species. To clarify this point, we examined ROS levels in HL60 cells subjected to PN-PDT pretreated with increasing concentrations (25-100 µM) of ascorbic acid, a natural antioxidant which act as a scavenger of superoxide radical anion ($O_2^{\bullet -}$) and hydroxyl radical ($HO^{\bullet}$) [30]. The results indicate that the intracellular ROS levels were reduced ~50% by 50 µM ascorbic acid (Fig. 3C) and that this antioxidant partially abolishes apoptotic cell death triggered by PN-PDT, as evidenced by an important reduction in the DNA cleavage (Fig. 3D). The fact that ascorbic acid did not decrease completely ROS levels, suggests that some radical oxygen species that are not reduced by the antioxidant, such as singlet oxygen ($^1O_2$), are also generated upon the photo-activation of PN[28,30]. To ascertain whether $^1O_2$ is generated by the photoactivation of PN, the cells were preincubated with increasing concentrations of sodium azide, a specific scavenger of $^1O_2$ [31]. As shown (Fig. 3E), sodium azide decreased in a concentration-dependent manner the ROS levels in cells exposed to PN-PDT. This is consistent with our previous results and it suggests that $O_2^{\bullet -}$, $HO^{\bullet}$ and $^1O_2$ probably are generated by PN-PDT, and indicates that PN behaves as a type I as well as and type II PS [28].

Involvement of the mitochondrial pathway in the PN-PDT-induced apoptosis

Mitochondria are organelles that play a pivotal role in cell signalling, integrating survival and cell death [32,33]. Mitochondria are also key targets of ROS generated by numerous PSs that induce cell death mainly through an apoptotic mechanism [34,35]. Therefore, we examined whether mitochondria are involved in PN-PDT-induced apoptosis on HL-60 cells. For this purpose, we analyzed the mitochondrial transmembrane potential ($\Delta\Psi_m$) since numerous physiological and pathological stimuli trigger an increase in the inner mitochondrial membrane permeability and the consequent dissipation of $\Delta\Psi_m$ [36]. The flow cytometry studies using the fluorescent probe JC-1 revealed that PN-PDT promotes dissipation of the $\Delta\Psi_m$ (Fig. 4A). This effect was early detected after light exposure (1 h) and the percentage of cells with low $\Delta\Psi$m in response to PN-PDT increased in a time dependent-fashion. Four hours after exposure to light, the percentage of cells with low $\Delta\Psi$m was ~70%, a 30-fold increase as compared to the control (Fig. 4B).

A consequence of an increase in the permeability of mitochondrial membranes is the release of apoptogenic factors, located in the mitochondrial intermembrane space, towards the cytosol. To determine whether cytochrome c is released from mitochondria to cytosol in response to PN-PDT, the levels of this proapoptotic factor were determined by immunoblot assay. As shown in Fig. 4C, cytochrome *c* was detected in the cytosolic fraction from cells treated with PN-PDT after a short time period of recovery (2 h) and its levels increased with the incubation time. Maximum levels of cytochrome c in the cytosol were observed 4 h after light exposure and accompanied by a parallel reduction in the mitochondrial levels. Together, these results indicate that PN-PDT activate the intrinsic pathway of apoptosis in HL-60 cells, causing mitochondrial membrane depolarization and cytochrome c release from mitochondria.

Caspase-3 and -9, are usually activated in response to numerous PS that focus their actions on the mitochondria. Thus, the role of executer caspase-3 on PN-PDT-induced apoptosis was evaluated by using the specific caspase-3 inhibitor z-DEVD-fmk. As shown in Fig. 5A, when HL-60 cells were preincubated with the inhibitor, the percentage of hypodiploid cells induced by PN-PDT decreased in a concentration-dependent manner. Apoptotic cell death was completely suppressed in presence of the higher concentration of the inhibitor (100 μM), suggesting that caspase-3 is the primary executioner caspase involved in the PN-PDT-induced apoptosis. No impact on the percentage of hypodiploid cells was detected when the cells were treated only with z-DEVD-fmk (data not shown). Because caspase-3 activation is an event prior to DNA fragmentation and PN-PDT induces significant DNA fragmentation at 4 h (see Fig. 2C), we measured caspase-3 activity before to that time. Cytosolic fractions from HL-60 cells treated with PN-PDT at different times were assayed for cleaving of the tetrapeptide Ac-DEVD-pNA, a specific substrate of caspase-3. As shown in Fig. 5B, PN-PDT induced caspase-3 activity in a time dependent-fashion. This was detected 1h after photosensitization and increased progressively along the incubation time. Consistent with above result, the pretreatment of the

cells with ascorbic acid (50 μM) or with the specific inhibitor of caspase-9 LEHD-CHO (50 μM) reduced PN-PDT-stimulated caspase-3 activity (Fig. 5B). These results suggest that PN-PDT-generated ROS induces apoptosis by caspase-3 activation through mitochondrial intrinsic pathway. Since the initiator caspase-9 is key to activate caspase-3, we next evaluated the caspase-9 activity after PN-PDT and in the presence of ascorbic acid. Cytosolic fractions from HL-60 cells treated with PN-PDT at 2 and 4 hours were assayed for cleaving of Ac-LEHD-pNA, a specific substrate of caspase-9. As shown in Fig 5C, PN-PDT induced caspase-9 activity since 2 h of treatment. In addition, the pretreatment of the cells with ascorbic acid (50 μM) reduced drastically PN-PDT-stimulated caspase-9 activity at all assayed times, which indicates that intrinsic pathway is activated by PN-PDT-generated ROS. Nevertheless, a total lack of caspase-3 activity after 4h post-PN-PDT was not observed with the pretreatment with LEHD-CHO, which indicates that caspase-3 could be also activated through alternative apoptotic pathways.

Caspase-8 activation is critical for PN-PDT-induced apoptosis

It has been reported that the photodynamic treatments may activate caspase-8 prior to the induction of apoptosis. This initiator caspase can directly activate caspase-3 through the so-called extrinsic pathway or indirectly via activation of the intrinsic pathway. In order to elucidate whether caspase-8 was implicated in the PN-PDT-induced apoptosis, cytosolic fractions were assayed for cleaving of the tetrapeptide Ac-IETD-pNA, a specific substrate for caspase-8. As shown in Fig. 6A, PN-PDT induced caspase-8 activity 1h after photosensitization and increased progressively along the incubation time. Consistent with this result, the specific inhibitor for caspase-8 z-IETD-fmk reduced, in a concentration-dependent manner, the percentage of apoptotic cells detected in response to PN-PDT (Fig. 6B). A reduction of ~80% in the frequency of apoptotic cells was observed with the higher concentration of the inhibitor used (200 μM). No impact on basal apoptosis was observed in cells incubated only with z-IETD-fmk (data not shown). We also analyzed the significance of caspase-8 on the activity of caspase-3 triggered by PN-PDT. As shown in the Fig. 6C, caspase-3 activity was notably inhibited (~70%) in presence of z-IETD-fmk (200 μM), confirming that the activation of caspase-3 by caspase-8 is an essential event in PN-PDT-induced apoptosis.

The activation of caspase-3 by the initiator caspase-8 (see Fig. 6C) and the lack of a total inhibition of caspase-3 activity when the cells were pretreated with the specific inhibitor of caspase-9 (see Fig. 5B), suggest a direct activation of caspase-3 by caspase-8. However, caspase-8 can also address the signal toward the mitochondria, activating the intrinsic pathway. To clarify this point, we analyzed caspase-9 activity and $\Delta\Psi_m$ after pretreatment of cells with the caspase-8 inhibitor z-IETD-fmk. After 4 h PN-PDT, both caspase-9 activity (Fig. 6D) and dissipation of the mitochondrial transmembrane potential (Fig. 6E) were abrogated when the cells were preincubated with z-IETD-fmk, indicating that caspase-8 activation by PN-PDT is key to induce the intrinsic pathway. We next examined whether caspase-8 activates the

mitochondrial pathway through Bid protein translocation, a proapoptotic member of the Bcl-2 family and a well-characterized caspase-8 substrate which is cleaved into an active form (i.e., truncated Bid [tBid]) and plays a key role as a link between the extrinsic and intrinsic pathways of apoptosis. Therefore, cytosolic and mitochondrial fractions obtained from HL-60 cells treated with PN-PDT were subjected to immunoblot analysis with antibodies which recognize the processed caspase-8 fragments or the truncated Bid protein. As shown in Fig. 6E, and in accordance with above results, a significant increase in processed caspase-8 was observed in the cytosolic fraction 1 hour after PN-PDT and increased progressively along the incubation time. Simultaneously, PN-PDT induced Bid cleavage mediated by caspase-8 activation, as demonstrated by the presence of tBid in the mitochondrial fraction. Maximum levels of tBid were observed at 2 h and the protein remained elevated for at least 4 h. The pretreatment of HL-60 cells with the caspase-8 inhibitor decreased the translocation of tBid to the mitochondrion in response to PN-PDT (Fig. 6F), confirming that caspase-8 mediates Bid cleavage in PN-PDT-induced apoptosis. Taken together, these results suggest that caspase-8 led the apoptosis through the mitochondrial intrinsic pathway by tBid induction and through the extrinsic pathway activating directly caspase-3. The failure of caspase-8 inhibitor to prevent completely the development of apoptosis, the caspase-3 activity and the mitochondrial transmembrane potential induced by PN-PDT, suggests that others signalling pathways can be implicated in the induction of apoptosis by PN-PDT.

PN-PDT activates intracellular signalling pathways with opposite effects on the cellular viability

It is known that PDT is able to activate signalling pathways implicated in apoptosis and cell survival, such as MAPKs (ERK1/2, P38-MAPK and JNK) or PI3K/Akt. To test whether these pathways are involved in PN-PDT-induced apoptosis, HL-60 cells were pretreated with specific inhibitors of these kinases and the apoptotic cells determined by flow cytometry. As shown in Fig. 7A, the percentage of hypodiploid cells detected in response to PN-PDT treatment diminished in presence of P38-MAPK inhibitor SB203580 (32% vs. 22%), whereas it augmented in presence of JNK inhibitor SP600125 (32% vs. 48%) and PI3K inhibitor LY2940002 (32% vs. 47%). No effect was appreciated when the cells were cultured in presence of PD98059, a specific inhibitor of mitogen-activated extracellular kinase 1/2 (MEK1/2) that is used to block the activation of ERK1/2. In consonance with the above results, the activity of caspase-3 increased by the pretreatment with SP600125 and LY2940002, and diminished with the inhibitor SB203580 (Fig. 7B). On the other hand, the inhibitor PD98059 did not have any impact on caspase-3 activity triggered by PN-PDT. Together, these results suggest that PN-PDT-induced apoptosis is modulated positively by p38-MAPK and negatively by JNK and PI3K/Akt, while ERK1/2 does not play any role.

Taking into account that cell death was detected 2-4 h after PN-PDT treatment (see Fig. 2E), the changes in the phosphorylation state of the above kinases was analyzed prior to that time, at the 2-60 min period. For this purpose, the cells were harvested at different times after

light exposure and p38-MAPK, JNK and Akt were analyzed by Western blot using antibodies that recognize the phosphorylated (activated) forms of each kinase. As shown in Fig. 7C, irradiation of HL-60 cells in presence of PN resulted in a quick increase (<2 min) in the phosphorylation of p38-MAPK, JNK and Akt. Although phosphorylation of p38-MAPK and JNK remained in phosphorylated stated at least 60 min, the signal of phospho-Akt decayed after de 15 min. As expected, due to its function in cell survival, phospho-Akt was also detected in lysates from control cells. Equivalent levels of total p38-MAPK, JNK and Akt were detected between experimental groups, indicating that the increasing in the levels of phosphorylation induced by PN-PDT was not due to changes in the expression of the kinases. Together, these results indicate that PN-PDT simultaneously actives intracellular signalling pathways with opposite effects on apoptosis. Thus, p38-MAPK acts as a death signal since it plays a significant role in PN-PDT-induced apoptosis, while JNK and PI3K/Akt act as survival signals.

Activation of P38-MAPK by PN-PDT triggers apoptosis through the mitochondrial pathway but independently of caspase-8

Because the intrinsic pathway is critical in the activation of apoptosis by PN-PDT in HL-60 cells, we determine whether p38-MAPK, JNK and Akt display a regulatory role on mitochondrial function. For this purpose, the cells were pretreated for 1h with the specific inhibitors of these kinases and $\Delta\Psi_m$ was analyzed by flow cytometry after the photodynamic treatment. Consistent with the effect on apoptosis and on caspase-3 activity (see Fig. 7A,B), mitochondrial membrane depolarization triggered by PN-PDT was partially abrogated by p38-MAPK inhibitor SB203580 and strongly enhanced by JNK inhibitor SP600121 (Fig. 8A). In contrast, PI3K inhibitor LY2940002 had not effect on $\Delta\Psi_m$. These results indicate that p38-MAPK and JNK, but not PI3K/Akt, activated by PN-PDT act through the mitochondria.

Taking into account that apoptosis induced by PN-PDT is initiated by caspase-8 activation, we further investigated the regulatory relationship between p38-MAPK and JNK with signalling pathways upstream of mitochondrion. To determinate the role of these kinases on caspase-8 activity and Bid translocation to mitochondria, HL-60 cells were treated with inhibitors of p38-MAPK or JNK before PN-PDT. The results indicate that inhibition of JNK enhanced significantly caspasa-8 activity (Fig. 8B) and, consequently, the levels of the active form of Bid (Fig. 8C). Nevertheless, inhibition of p38-MAPK did not have any effect on caspase-8 activity neither on t-Bid levels. These results suggest that although JNK and p38-MAPK drive through the mitochondria the activated signals by PN-PDT, only JNK acts upstream of mitochondria by means of caspase-8 activation and Bid translocation. Together, these results indicate that PN behaves as an efficient type I as well as and type II PS able to generate ROS and to activate p38-MAPK and caspase-8. This activation is enough to induce apoptosis through the intrinsic and extrinsic signalling pathways despite survival signals (Akt and JNK) are also activated by PN-PDT.

Discussion

Apoptosis is a crucial event extremely regulated in multiple physiological processes, and its loss of control underlies to many clinical pathologies including cancer. PDT, a treatment modality for many cancer types and for certain non-malignant diseases, has been shown to induce apoptosis of cancer cells both *in vitro* and *in vivo* [10]. PDT might become a major weapon to treat cancer but the small number of molecules known that behave as efficient photosensitizers limit the potential of this treatment. In this study, we evaluate the effectiveness of PN as PS to exert PDT-mediated apoptosis on tumor cells and subsequently we investigate its mechanism of action. The experimental results presented clearly show to PN as a potential PS agent in PDT for the cancer treatment.

It is well known that PN is an efficient $^1O_2$ PS in no biological systems due to its excellent quantum yield, close to unity in solvents of very different polarity [17,37]. In addition, it has good photostability under the irradiation of light and low ability to deactivate $^1O_2$. Also, enhanced antiparasitic activity by light is exhibited in many natural products based on the PN skeleton that have been isolated from plants [20]. However, photobiological studies with PN on tumor cells have not been performed to date. Our results demonstrate that PN, in presence of light, induces cell death of human tumor-derived cell lines and it does not display toxicity, with the maximum dose employed, in absence of light. In addition, citotoxicity due to PN-PDT depends on concentration of PN and light employed suggesting that PN behaves as an efficient photosensitizer. However, the level of sensibility of the cell lines to PN-PDT was different, being HL60 the most sensitive. This could be due to several factors such as differences in the activation of repairing mechanisms of the cell, permeability of cell membranes or intracellular localization of PN [2].

In PDT the induction of cell death through apoptosis is preferred over necrosis for several reasons. Apoptosis can be activated with low doses of irradiation, it does not trigger an exacerbated inflammatory process as side effect and it stimulates the host immune response. The induction of apoptosis may be determined by multiple factors such as the photochemical mechanism (type I or II) or the cell type, although the subcellular localization, the concentration of photosensitizer and the dose of light are the most deciding parameters [2,4,8,14]. In this way, 5 μM of PN and a light dose of 20 J/cm^2 promoted ~50% of HL-60 cell death 24 hours after PN-PDT. This aspect is important to induce apoptosis by the photodynamic treatment, the damage must be enough severe to avoid cell repairing but sufficiently mild to produce energy, otherwise the cell will die through necrosis. In our experiments, the percentage of cells that exhibit some early hallmark of apoptosis raised significantly since 2-4 hours, reaching ~50% at 6 hours after the treatment, which indicates that PN-PDT is a potent and rapid inductor of apoptosis.

We also demonstrate that PN-PDT induces ROS generation and that these chemical species are involved in the cell death since ascorbic acid reduced its levels and partially blocked apoptosis. Failure of this antioxidant to prevent completely the apoptosis induced by PN-PDT appear to be consequence of its inability to scavenge all the ROS generated. It is well known that ascorbic acid is a good scavenger of $O_2^{\bullet -}$ and $HO^{\bullet}$, both generated in type I reaction mechanism, and in lesser extent of $^1O_2$ generated in type II reaction mechanism [30]. It is for this reason that PN-PDT can be generating $^1O_2$ by a type II mechanism in addition to the ROS generated in type I. This is supported by the fact that sodium azide, a specific scavenger of $^1O_2$, reduces the generation of ROS by PN-PDT. Although, the H_2DCFDA is not oxidized by $^1O_2$, the effect of azide on ROS levels may be explained because peroxy products and peroxyl radicals are yielded from interaction of singlet oxygen with different biomolecules [38]. In accordance with the photophysical and photochemical data of the PN, the generation of $^1O_2$ could be the triggering factor that lead up the cell to the apoptosis. However, we cannot exclude the possibility that $O_2^{\bullet -}$ is also formed together to $^1O_2$ in PN-PDT. This is consistent with the results of Espinoza et al. [39], who prove that phenanelone behaves like a type I as well as type II photosensitizer.

A common feature of apoptosis initiated by the PDT is the acute stress response through the generation of ROS, causing a rapid release of cytochrome c from the mitochondria to the cytosol and caspase-9 activation [14]. The data shown in this work suggest that mitochondrion is a target for ROS generated by PN-PDT. Depolarization of the mitochondrial membrane by PN-PDT and the consequent release of cytochrome c was an early event (2h), indicating that ROS rapidly cause mitochondrial damage. Furthermore, the blockage of apoptotic cell death caused by inhibition of caspase-3 is in accordance with several studies which prove that many photosensitizers activate the intrinsic pathway and caspase-3 to execute the apoptotic process [4]. The direct relationship between ROS generation and caspase-9 and -3 activation was established using ascorbic acid, which proves that mitochondrial intrinsic pathway is induced by PN-PDT-generated ROS. Although the blockage of caspase-3 activity was not total, it is in accordance with a decrease of ROS levels (50%) and supports the idea that PN generates $^1O_2$, a radical that is not reduced by the ascorbic acid.

All data present herein demonstrate the involvement of the intrinsic pathway in the PN-PDT-induced apoptosis; however, the inability of caspase-9 inhibitor to prevent completely caspase-3 activity suggest that this executer caspase is also activated independently of intrinsic pathway. Several studies on PDT have revealed that the activation and mobilization of death receptors stimulates caspase-3 activity through the activation of caspase-8 [9,40]. Interestingly, we found that generation of ROS and the consequent induction of apoptosis by PN-PDT is accompanied by a quick activation (1h) of caspase-8. Besides, we demonstrated that the inhibition of this activity decreases drastically the percentage of apoptotic cells and caspase-3 activity, indicating that direct activation of caspase-3 by caspase-8 is important for the cell death

induced by PN-PDT. It is widely known that the proapoptotic protein Bid can connect to both intrinsic and extrinsic apoptotic pathways [41]. In this way, we have not only shown that cytosolic Bid undergoes proteolysis in the HL-60 cells exposed to PN-PDT but also that this is induced by caspase-8 activation. This finding is in accordance to the earlier work of Zhuang *et al* [42], which demonstrates hydrolysis of Bid and caspase-8 activation in response to $^1O_2$ generated by photosensitization of HL-60 cells with rose Bengal. Also, it is interesting to underline, in our study, that caspase-8 activation is detected subsequently to the early detection of ROS (30min) but before the depolarization of mitochondrial membrane, cytochrome c release, caspase-9 and -3 activation. Our results -consistent with work of Zhuang et al- lead us to argue that PN-PDT-generated ROS possibly could be activating caspase-8 and consequently to provoke the mitochondrial depolarization. This is supported by the fact that the dissipation of mitochondrial transmembrane potential is also blocked by the inhibition of this caspase. In addition, in absence of light PN did not display cytotoxicity neither activated caspase-8, consequently we could assume that changes on caspase-8 activity produced by PN-PDT are likely caused by ROS generation.

A stage where are activated extrinsic and mitochondrial pathways in response to an apoptotic stimulate has been shown previously in the cells known as type II [43,44]. In these cells, caspase-8 is not sufficient to trigger the apoptosis through the direct activation of caspase-3, as a result the mitochondria is used as organelle amplifier of the apoptotic signal. On the other hand, the failure of caspase-8 inhibitor to prevent completely mitochondrial depolarization, caspase-3 activity and apoptosis induced by PN-PDT, suggests that other signaling pathways may be implicated in the activation of mitochondrial pathway. We find that cell stress (p38-MAPK and JNK) and survival (PI3K/Akt) pathways, which are susceptible of modulation by ROS [4,45], are activated by the PN-PDT on HL60 cells. These kinases are activated earlier than caspase-8, which could indicates initially that p38-MAPK, JNK and Akt act upstream of mitochondrial pathway.

Inhibition of p38-MAPK block partially mitochondrial depolarization, caspase-3 activity and apoptosis induced by PN-PDT, which is consistent with the report of Zhuang et al [42]. However, the inability of p38-MAPK inhibitor to prevent caspase-8 and Bid activation induced by PN-PDT suggests that p38-MAPK signaling converge on the mitochondria, independently of caspase-8. In this way, p38-MAPK is able to phosphorylate the pro-apoptotic protein BAX, causing its translocation from cytosol to the mitochondria, and also the anti-apoptotic proteins Bcl-X_L and Bcl-2, preventing they accumulate into the mitochondrial membrane [46,47]. Surprisingly, the inhibition of JNK increases activity of caspase-8 and translocation of Bid, and enhances mitochondrial depolarization, caspase-3 activity and apoptosis, revealing an anti-apoptotic role of JNK in PN-PDT and suggesting that this kinase acts upstream of mitochondria, through caspase-8. This is reinforced by the fact that phosphorylation of JNK starts previously to the activation of caspase-8. *A priori*, these results could be in disagreement with a classical

pro-apoptotic role of JNK, however, PDT studies on gastrointestinal tumor cells or on HeLa cells have proven that JNK protects to the cells from apoptosis [48,49].

We also find that the suppression of Akt activity enhances the apoptosis induced by PN-PDT, which is consistent with previous PDT reports that show a decrease of cell viability despite Akt is activated [50,51]. Moreover, it is known that PI3K/Akt pathway activation modulates negatively the apoptotic mitochondrial pathway through the phosphorylation and inactivation of proapoptotic protein Bad [52–54]. However, we do not observe inhibition of mitochondrial depolarization in the cells treated with the PI3K inhibitor prior PN-PDT, indicating that Akt acts downstream the mitochondria. Although the mechanism by which Akt inhibits the apoptotic cascade remains to be elucidated, previous studies show that Akt may induce expression of inhibitors of apoptosis proteins (IAPs) through phosphorylation and activation of NF-kB [55] or even it may directly phosphorylate and inactivate caspase-9 [13,56]. Further studies will be need to identify the molecular elements of cell death and survival pathways that are involved in the PN-PDT.

Because of the optical properties of tissues, red light is preferred in PDT since longer wavelengths have better penetration in tissues. Although the broadband white light used to carry out PN-PDT was sufficient to induce apoptosis on cancer cells, the absorbance of PN does not extend beyond 450 nm, wavelength that not penetrate in tissues beyond 0.5 millimeters depth. Therefore, for an ideal PDT, it would be necessary to prepare analogs or to isolate compounds derived from plants, based on PN moiety, with longer wavelength absorbance profiles. However, this not must be an impediment to apply PN-PDT *in vivo*, since the use of white light source after intravesicular administration of 5-aminolevulinic acid (5-ALA) have achieved to eliminate urothelial carcinoma [57]. Protoporphyrin IX, synthesized from 5-ALA in the mitochondria, have a maximum peak of absorption at 410 nm and very smaller peaks near 510, 545, 580 and 630 nm. Moreover, it have been proven, *in vitro and in vivo,* that ALA-PDT using blue and white LEDs have greater antitumor effects compared to the red LEDs [58]. Regardless, PN might be used for treatment of superficial skin cancer or internal cancers as esophagus, lungs, stomach, or bladder that present affected superficial regions. Also, the use of shorter wavelength light might help to reduce the rate of severe side effects as transmural necrosis leading to perforation or stenosis via transmural fibrosis caused when red light is used [59].

In conclusion, the results obtained here provides solid evidences that oxidative stress generated by the PN-PDT induces apoptosis, on human tumor cells, through caspase-8 and p38-MAPK activation. This finding would supports future research directed to develop novel molecules based on PN moiety that improve the effectiveness of PDT in the treatment of cancer and others nononcological malignancies.

Acknowledgments

We thank Dr. Carlos Manuel Ruiz de Galarreta and Dr. Christopher Paetzold for comments and language editing. This work was supported in part by the Universidad de Las Palmas de Gran Canaria [Grant ULPGC2009-14].

References

1. Dougherty TJ, Gomer CJ, Henderson BW, et al. Photodynamic therapy. *J Natl Cancer Inst*. 1998;90(12):889-905.

2. Kessel D, Oleinick NL. Cell Death Pathways Associated with Photodynamic Therapy: an Update. *Photochem Photobiol*. November 2017. doi:10.1111/php.12857

3. Foote CS. Definition of type I and type II photosensitized oxidation. *Photochem Photobiol*. 1991;54(5):659.

4. Mroz P, Yaroslavsky A, Kharkwal GB, Hamblin MR. Cell Death Pathways in Photodynamic Therapy of Cancer. *Cancers*. 2011;3(2):2516-2539. doi:10.3390/cancers3022516

5. Castano AP, Mroz P, Hamblin MR. Photodynamic therapy and anti-tumour immunity. *Nat Rev Cancer*. 2006;6(7):535-545. doi:10.1038/nrc1894

6. Abels C. Targeting of the vascular system of solid tumours by photodynamic therapy (PDT). *Photochem Photobiol Sci Off J Eur Photochem Assoc Eur Soc Photobiol*. 2004;3(8):765-771. doi:10.1039/b314241h

7. Oleinick NL, Morris RL, Belichenko I. The role of apoptosis in response to photodynamic therapy: what, where, why, and how. *Photochem Photobiol Sci Off J Eur Photochem Assoc Eur Soc Photobiol*. 2002;1(1):1-21.

8. Almeida RD, Manadas BJ, Carvalho AP, Duarte CB. Intracellular signaling mechanisms in photodynamic therapy. *Biochim Biophys Acta BBA - Rev Cancer*. 2004;1704(2):59-86. doi:10.1016/j.bbcan.2004.05.003

9. Ali SM, Chee SK, Yuen GY, Olivo M. Photodynamic therapy induced Fas-mediated apoptosis in human carcinoma cells. *Int J Mol Med*. 2002;9(3):257-270.

10. Plaetzer K, Kiesslich T, Oberdanner CB, Krammer B. Apoptosis following photodynamic tumor therapy: induction, mechanisms and detection. *Curr Pharm Des*. 2005;11(9):1151-1165.

11. Buytaert E, Dewaele M, Agostinis P. Molecular effectors of multiple cell death pathways initiated by photodynamic therapy. *Biochim Biophys Acta*. 2007;1776(1):86-107. doi:10.1016/j.bbcan.2007.07.001

12. Xue L y, He J, Oleinick NL. Promotion of photodynamic therapy-induced apoptosis by stress kinases. *Cell Death Differ*. 1999;6(9):855-864. doi:10.1038/sj.cdd.4400558

13. Clerkin JS, Naughton R, Quiney C, Cotter TG. Mechanisms of ROS modulated cell survival during carcinogenesis. *Cancer Lett*. 2008;266(1):30-36. doi:10.1016/j.canlet.2008.02.029

14. Robertson CA, D. Hawkins Evans, Abrahamse H. Photodynamic therapy (PDT): a short review on cellular mechanisms and cancer research applications for PDT. *J Photochem Photobiol B*. 2009;96(1):1-8. doi:10.1016/j.jphotobiol.2009.04.001

15. Dougherty TJ, Gomer CJ, Henderson BW, et al. Photodynamic therapy. *J Natl Cancer Inst*. 1998;90(12):889-905.

16. Ormond AB, Freeman HS. Dye Sensitizers for Photodynamic Therapy. *Mater Basel Switz*. 2013;6(3):817-840. doi:10.3390/ma6030817

17. Schmidt R, Tanielian C, Dunsbach R, Wolff C. Phenalenone, a universal reference compound for the determination of quantum yields of singlet oxygen O2(1Δg) sensitization. *J Photochem Photobiol Chem*. 1994;79(1-2):11-17. doi:10.1016/1010-6030(93)03746-4

18. Martí C, Jürgens O, Cuenca O, Casals M, Nonell S. Aromatic ketones as standards for singlet molecular oxygen photosensitization. Time-resolved photoacoustic and near-IR emission studies. *J Photochem Photobiol Chem*. 1996;97(1-2):11-18. doi:10.1016/1010-6030(96)04321-3

19. Binks RH, Greenham JR, Luis JG, Gowen SR. A phytoalexin from roots of Musa acuminata var. pisang sipulu. *Phytochemistry*. 1997;45(1):47-49. doi:10.1016/S0031-9422(96)00796-0

20. Quiñones W, Escobar G, Echeverri F, et al. Synthesis and Antifungal Activity of Musa Phytoalexins and Structural Analogs. *Molecules*. 2000;5(7):974-980. doi:10.3390/50700974

21. Elsebai MF, Saleem M, Tejesvi MV, et al. Fungal phenalenones: chemistry, biology, biosynthesis and phylogeny. *Nat Prod Rep*. 2014;31(5):628. doi:10.1039/c3np70088g

22. Lazzaro A, Corominas M, Martí C, et al. Light- and singlet oxygen-mediated antifungal activity of phenylphenalenone phytoalexins. *Photochem Photobiol Sci*. 2004;3(7):706-710. doi:10.1039/B401294A

23. Rosquete LI, Cabrera-Serra MG, Piñero JE, et al. Synthesis and in vitro antiprotozoal evaluation of substituted phenalenone analogues. *Bioorg Med Chem*. 2010;18(12):4530-4534. doi:10.1016/j.bmc.2010.04.062

24. Gutiérrez D, Flores N, Abad-Grillo T, McNaughton-Smith G. Evaluation of substituted phenalenone analogues as antiplasmodial agents. *Exp Parasitol*. 2013;135(2):456-458. doi:10.1016/j.exppara.2013.08.008

25. Hölscher D, Dhakshinamoorthy S, Alexandrov T, et al. Phenalenone-type phytoalexins mediate resistance of banana plants (Musa spp.) to the burrowing nematode Radopholus similis. *Proc Natl Acad Sci U S A*. 2014;111(1):105-110. doi:10.1073/pnas.1314168110

26. Song R, Feng Y, Wang D, Xu Z, Li Z, Shao X. Phytoalexin Phenalenone Derivatives Inactivate Mosquito Larvae and Root-knot Nematode as Type-II Photosensitizer. *Sci Rep*. 2017;7:42058. doi:10.1038/srep42058

27. Späth A, Leibl C, Cieplik F, et al. Improving Photodynamic Inactivation of Bacteria in Dentistry: Highly Effective and Fast Killing of Oral Key Pathogens with Novel Tooth-Colored Type-II Photosensitizers. *J Med Chem*. 2014;57(12):5157-5168. doi:10.1021/jm4019492

28. Espinoza C, Trigos Á, Medina ME. Theoretical Study on the Photosensitizer Mechanism of Phenalenone in Aqueous and Lipid Media. *J Phys Chem A*. 2016;120(31):6103-6110. doi:10.1021/acs.jpca.6b03615

29. Chen X, Zhong Z, Xu Z, Chen L, Wang Y. 2',7'-Dichlorodihydrofluorescein as a fluorescent probe for reactive oxygen species measurement: Forty years of application and controversy. *Free Radic Res*. 2010;44(6):587-604. doi:10.3109/10715761003709802

30. Hosaka S, Obuki M, Nakajima J, Suzuki M. Comparative study of antioxidants as quenchers or scavengers of reactive oxygen species based on quenching of MCLA-dependent chemiluminescence. *Lumin J Biol Chem Lumin*. 2005;20(6):419-427. doi:10.1002/bio.867

31. Bancirova M. Sodium azide as a specific quencher of singlet oxygen during chemiluminescent detection by luminol and Cypridina luciferin analogues. *Lumin J Biol Chem Lumin*. 2011;26(6):685-688. doi:10.1002/bio.1296

32. Fulda S, Kroemer G. Mitochondria as therapeutic targets for the treatment of malignant disease. *Antioxid Redox Signal*. 2011;15(12):2937-2949. doi:10.1089/ars.2011.4078

33. Galluzzi L, Kepp O, Trojel-Hansen C, Kroemer G. Mitochondrial control of cellular life, stress, and death. *Circ Res*. 2012;111(9):1198-1207. doi:10.1161/CIRCRESAHA.112.268946

34. Circu ML, Aw TY. Reactive oxygen species, cellular redox systems, and apoptosis. *Free Radic Biol Med*. 2010;48(6):749-762. doi:10.1016/j.freeradbiomed.2009.12.022

35. Lu Z, Tao Y, Zhou Z, et al. Mitochondrial reactive oxygen species and nitric oxide-mediated cancer cell apoptosis in 2-butylamino-2-demethoxyhypocrellin B photodynamic treatment. *Free Radic Biol Med*. 2006;41(10):1590-1605. doi:10.1016/j.freeradbiomed.2006.08.021

36. Bonora M, Wieckowski MR, Chinopoulos C, et al. Molecular mechanisms of cell death: central implication of ATP synthase in mitochondrial permeability transition. *Oncogene*. 2015;34(12):1475-1486. doi:10.1038/onc.2014.96

37. Martí C, Jürgens O, Cuenca O, Casals M, Nonell S. Aromatic ketones as standards for singlet molecular oxygen O2(1Δg) photosensitization. Time-resolved photoacoustic and near-IR emission studies. *J Photochem Photobiol Chem*. 1996;97(1):11-18. doi:10.1016/1010-6030(96)04321-3

38. Bilski P, Belanger AG, Chignell CF. Photosensitized oxidation of 2′,7′-dichlorofluorescin: singlet oxygen does not contribute to the formation of fluorescent oxidation product 2′,7′-dichlorofluorescein. *Free Radic Biol Med*. 2002;33(7):938-946. doi:10.1016/S0891-5849(02)00982-6

39. Espinoza C, Trigos Á, Medina ME. Theoretical Study on the Photosensitizer Mechanism of Phenalenone in Aqueous and Lipid Media. *J Phys Chem A*. 2016;120(31):6103-6110. doi:10.1021/acs.jpca.6b03615

40. Schempp CM, Simon-Haarhaus B, Termeer CC, Simon JC. Hypericin photo-induced apoptosis involves the tumor necrosis factor-related apoptosis-inducing ligand (TRAIL) and activation of caspase-8. *FEBS Lett*. 2001;493(1):26-30.

41. Kalkavan H, Green DR. MOMP, cell suicide as a BCL-2 family business. *Cell Death Differ*. October 2017. doi:10.1038/cdd.2017.179

42. Zhuang S, Demirs JT, Kochevar IE. p38 mitogen-activated protein kinase mediates bid cleavage, mitochondrial dysfunction, and caspase-3 activation during apoptosis induced by singlet oxygen but not by hydrogen peroxide. *J Biol Chem*. 2000;275(34):25939-25948. doi:10.1074/jbc.M001185200

43. Fesik SW. Promoting apoptosis as a strategy for cancer drug discovery. *Nat Rev Cancer*. 2005;5(11):876-885. doi:10.1038/nrc1736

44. Prado-Garcia H, Romero-Garcia S, Morales-Fuentes J, Aguilar-Cazares D, Lopez-Gonzalez JS. Activation-induced cell death of memory CD8+ T cells from pleural effusion of lung cancer patients is mediated by the type II Fas-induced apoptotic pathway. *Cancer Immunol Immunother*. 2012;61(7):1065-1080. doi:10.1007/s00262-011-1165-5

45. Castano AP, Demidova TN, Hamblin MR. Mechanisms in photodynamic therapy: part two—cellular signaling, cell metabolism and modes of cell death. *Photodiagnosis Photodyn Ther*. 2005;2(1):1-23. doi:10.1016/S1572-1000(05)00030-X

46. Farley N, Pedraza-Alva G, Serrano-Gomez D, et al. p38 mitogen-activated protein kinase mediates the Fas-induced mitochondrial death pathway in CD8+ T cells. *Mol Cell Biol*. 2006;26(6):2118-2129. doi:10.1128/MCB.26.6.2118-2129.2006

47. Kim B-J, Ryu S-W, Song B-J. JNK- and p38 kinase-mediated phosphorylation of Bax leads to its activation and mitochondrial translocation and to apoptosis of human hepatoma HepG2 cells. *J Biol Chem*. 2006;281(30):21256-21265. doi:10.1074/jbc.M510644200

48. Xia HH-X, He H, De Wang J, et al. Induction of apoptosis and cell cycle arrest by a specific c-Jun NH2-terminal kinase (JNK) inhibitor, SP-600125, in gastrointestinal cancers. *Cancer Lett*. 2006;241(2):268-274. doi:10.1016/j.canlet.2005.10.031

49. Assefa Z, Vantieghem A, Declercq W, et al. The activation of the c-Jun N-terminal kinase and p38 mitogen-activated protein kinase signaling pathways protects HeLa cells from apoptosis following photodynamic therapy with hypericin. *J Biol Chem*. 1999;274(13):8788-8796.

50. Bozkulak O, Wong S, Luna M, et al. Multiple components of photodynamic therapy can phosphorylate Akt. *Photochem Photobiol*. 2007;83(5):1029-1033. doi:10.1111/j.1751-1097.2007.00137.x

51. Wan J, Wu W, Che Y, Kang N, Zhang R. Low dose photodynamic-therapy induce immune escape of tumor cells in a HIF-1α dependent manner through PI3K/Akt pathway. *Int Immunopharmacol*. 2015;28(1):44-51. doi:10.1016/j.intimp.2015.05.025

52. Szanto A, Bognar Z, Szigeti A, Szabo A, Farkas L, Gallyas F. Critical role of bad phosphorylation by Akt in cytostatic resistance of human bladder cancer cells. *Anticancer Res*. 2009;29(1):159-164.

53. Bozkulak O, Wong S, Luna M, et al. Multiple components of photodynamic therapy can phosphorylate Akt. *Photochem Photobiol*. 2007;83(5):1029-1033. doi:10.1111/j.1751-1097.2007.00137.x

54. Son D, Na YR, Hwang E-S, Seok SH. Platelet-derived growth factor-C (PDGF-C) induces anti-apoptotic effects on macrophages through Akt and Bad phosphorylation. *J Biol Chem*. 2014;289(9):6225-6235. doi:10.1074/jbc.M113.508994

55. Duronio V. The life of a cell: apoptosis regulation by the PI3K/PKB pathway. *Biochem J*. 2008;415(3):333-344. doi:10.1042/BJ20081056

56. Li P, Zhou L, Zhao T, et al. Caspase-9: structure, mechanisms and clinical application. *Oncotarget*. 2017;8(14):23996-24008. doi:10.18632/oncotarget.15098

57. Waidelich R, Beyer W, Knchel R, et al. Whole bladder photodynamic therapy with 5-aminolevulinic acid using a white light source. *Urology*. 2003;61(2):332-337. doi:10.1016/S0090-4295(02)02164-7

58. Hatakeyama T, Murayama Y, Komatsu S, et al. Efficacy of 5-aminolevulinic acid-mediated photodynamic therapy using light-emitting diodes in human colon cancer cells. *Oncol Rep*. 2013;29(3):911-916.

59. Mordon S, Maunoury V. Using white light during photodynamic therapy: visualization only or treatment? *Eur J Gastroenterol Hepatol*. 2006;18(7):765-771. doi:10.1097/01.meg.0000223910.08611.79

Figure legends

Figure 1. Effect of PN-PDT on cell viability. (A) Chemical structure of Phenalenone. (B) Photoactivation of PN decreases cell viability in HL-60, A431 and A549 cells. The cells were incubated for 30 min with the indicated concentrations of PN before exposure to light (20 J cm^{-2}). Cell viability was determined 24 h after light exposure by the MTT assay. Data represent the mean of three experiments each performed by triplicates. Cells treated with vehicle, V, or with 30 μM PN in absence of light exposure, C, were used as controls. (C) Phototoxicity of PN is dependent of light fluence. HL-60 cells were cultured for 30 min with the specified concentrations of PN before exposure to light (5, 15 and 20 J cm^{-2}). Cell viability was evaluated 24 h following exposure to light. Non irradiated cells treated with 30 μM PN were used as control. Data represent the mean of three experiments each performed by triplicates. (D) Phototoxicity is dependent of light exposure length. HL-60 cells were incubated for 30 min with PN before exposure to 11 mW cm^{-2} of light intensity for the indicated time periods. The cells were allowed to recover for 24 h and cell viability was measured by the MTT assay. Data represent the mean of three experiments each performed by triplicates. Cells treated with 30 μM PN but not exposed to light were used as control.

Figure 2. PN-PDT induces apoptotic cell death in HL-60 cells. (A) The cells were incubated with 5 μM PN in absence (control) or presence of light (PDT; fluence: 20 J cm^{-2}) and allowed to recover for 6 h. The cells were collected, stained with bisbenzimide trihydrochloride and visualized by fluorescent microscopy; photomicrographs of representative fields of cells to evaluate nuclear chromatin condensation (i.e., apoptosis) are shown. (B) The cells were treated as above and apoptotic nuclei were quantified by fluorescent microscopy at the indicated time periods after PDT. *P<0.05 compared to control. (C) Effect on DNA fragmentation assessed by agarose gel electrophoresis (D) The cells were harvested 6 h after PN-PDT and cell distribution according to their DNA content was determined by flow cytometry using the propidium iodide staining procedure; the position of cells with hypodiploid (Sub-G_1) DNA content (i.e., apoptotic cells) is indicated by a dotted line. Representative histograms are shown. (E) Quantitation of hypodiploid cells as a function of time after PN-PDT. *P<0.05 compared to control, C.

Figure 3. PN-PDT induces ROS generation in HL-60 cells. (A) The cells were incubated with H_2-DCF and the indicated concentrations of PN in absence (control, C) or presence of light (fluence: 20 J cm^{-2}) for 30 min, and harvested immediately after light exposure. The fluorescence of oxidized H_2-DCF was determined by flow cytometry. A representative histogram (n=3) is shown. (B) ROS levels were determined as above and bar graph represents the median of oxidized H_2-DCF fluorescence. **P*<0.05 compared to control. (C) Effect of increasing concentrations of ascorbate (Asc) on intracellular ROS levels determined immediately after PN-PDT (fluence: 20 J cm^{-2}). The bar graph represents the median of oxidized H_2-DCF fluorescence. **P*<0.05 compared to control, C; $^{\#}$*P*<0.05 compared to ascorbate untreated group. (D) Ascorbate reduces DNA fragmentation in cells subjected to PN-PDT (fluence: 20 J cm^{-2}) after 6h of light exposure. (E) Effect of sodium azide on intracellular ROS levels, determined by flow cytometry immediately after light exposure (fluence: 20 J cm^{-2}). The bar graph represents the median of oxidized H_2-DCF fluorescence. **P*<0.05 compared to control, C; $^{\#}$*P*<0.05 compared to azide untreated group.

Figure 4. PN-PDT induces mitochondrial membrane potential dissipation and cytochrome c release from mitochondria in HL-60 cells. (A) The cells were incubated with 5 μM PN in absence (control) or presence of light (fluence: 20 J cm^{-2}) and allowed to recover for 4 h. Mitochondrial transmembrane potential was evaluated by flow cytometry after staining with the fluorescent probe JC-1; the value into the right low square represents the percentage of cells with a low $\Delta\Psi_m$. A representative histogram (n=3) is shown. (B) The cells were treated as above and harvested at the indicated time points after PN-PDT. **P*<0.05 compared to control. (C) Cytosolic and mitochondrial levels of cytochrome c were determined as a function of time after exposure to light (fluence: 20 J cm^{-2}) by western blot; COX IV was used as a loading control. A representative western blot (n=3) is shown.

Figure 5. PN-PDT-generated ROS activates caspase-3 and caspase-9 in HL-60 cells. (A) The cells were pre-incubated with the indicated concentrations of z-DEVD-fmk for 1 h and then exposed to 5 μM PN in absence (control) or presence of light (fluence: 20 J cm^{-2}). The cells were harvested 4 h after irradiation and cell distribution according to their DNA content was

determined by flow cytometry using the propidium iodide staining procedure. *P<0.05 compared to control, C; $^{\#}$P<0.05 compared to z-DEVD-fmk untreated group. (B) Effect of ascorbate and LEHD-CHO on caspase-3 activity in cells subjected to PN-PDT. The cells were pre-incubated with 50 μM ascorbate, 50 μM of caspase-9 inhibitor LEHD-CHO or vehicle for 1 h and harvested at the indicated time points after PN-PDT. Caspase-3 activity was determined from lysates using the specific colorimetric substrate Ac-DEVD-pNA. (C) Effect of ascorbate on caspase-9 activity in cells subjected to PN-PDT. The cells were pre-incubated with 50 μM ascorbate, or vehicle for 1 h and harvested at the indicated time points after PN-PDT. Caspase-9 activity was determined from lysates using the specific colorimetric substrate Ac-LEHD-pNA. *P<0.05 compared to control, C; $^{\#}$P<0.05 compared to vehicle-treated alone.

Figure 6. Caspase-8 is activated by PN-PDT and induces proteolytic cleavage of Bid in HL-60 cells. (A) The cells were incubated with 5 μM PN in absence (control) or presence of light (fluence: 20 J cm^{-2}) and allowed to recover for the indicate time points. Caspase-8 activity was determined from lysates using the specific colorimetric substrate Ac-IETD-pNA. *P<0.05 compared to control. (B, C, D, E) Inhibition of caspase-8 activity blocks apoptosis, caspase-3 activity, caspase-9 activity and mitochondrial potential dissipation triggered by PN-PDT. The cells were pre-incubated with the specified concentrations of caspase-8 inhibitor z-IETD-fmk for 1 h, then subjected to 5 μM PN in absence (control) or presence of light (fluence: 20 J cm^{-2}) and harvested 4 h after light exposure. Hypodiploid cells were determined by flow cytometry using the propidium iodide staining procedure, caspase-3 activity was evaluated from lysates using Ac-DEVD-pNA as colorimetric substrate, caspase-9 activity was evaluated from lysates using Ac-LEHD-pNA as colorimetric substrate and $\Delta\Psi_m$ was analyzed by flow cytometry after staining with the fluorescent probe JC-1. *P<0.05 compared to control; $^{\#}$P<0.05 compared to z-IETD-fmk untreated group. (E) PN-PDT induces proteolytic cleavage of caspase-8 and Bid. Levels of active caspase-8 (cytosolic fractions) and t-Bid (mitochondrial fractions) were analyzed by western blot. COX-IV was used as a loading control. A representative western blot (n=3) is shown. (F) Inhibition of caspase-8 blocks cleavage of Bid triggered by PN-PDT. The cells were pre-incubated with the indicated concentrations of z-IETD-fmk for 1 h and then subjected to 5 μM PN in absence (control) or presence of light (fluence: 20 J cm^{-2}), and harvested 2 h after

light exposure. Mitochondrial fractions were analyzed by western blot to determine the levels of tBid. COX-IV was used as a loading control. A representative western blot (n=3) is shown.

Figure 7. P38-MAPK, JNK and Akt are activated in response to PN-PDT in HL-60 cells. (A, B) The cells were pre-incubated with 10 μM SB203580 (SB, p38-MAPK inhibitor), 1 μM SP600125 (SP, JNK inhibitor), 5 μM PD98059 (PD, MEK1 inhibitor), 20 μM LY294002 (LY, Akt inhibitor) or vehicle (V) for 1 h and then treated with 5 μM PN in presence of light (fluence: 20 J cm^{-2}). Non irradiated cells treated with 5 μM PN were used as control, C. Four hours after light exposure, hypodiploid cells were determined by flow cytometry using the propidium iodide staining method, and caspase-3 activity was evaluated from lysates using Ac-DEVD-pNA as colorimetric substrate. *P<0.05 significantly different from control. $^{\#}$P<0.05 compared to vehicle (C) The cells were incubated with 5 μM PN in absence (control) or presence of light (fluence: 20 J cm^{-2}) and harvested at the indicate time points after PN-PDT. Protein extracts were prepared and analyzed by western blot with specific antibodies to ascertain the phosphorylation of p38-MAPK, JNK and Akt. Membranes were stripped and reprobed with total p38-MAPK, JNK and Akt antibodies as loading controls. A representative western blot (n=3) is shown.

Figure 8. Effect of MAPKs inhibitors on mitochondrial transmembrane potential and on caspase-8 activity in HL-60 cells. (A) The cells were pre-incubated with 10 μM SB203580 (SB, p38-MAPK inhibitor), 1 μM SP600125 (SP, JNK inhibitor), 20 μM LY294002 (LY, Akt inhibitor) or vehicle (V) for 1 h, and then cultured with 5 μM PN in presence of light (fluence: 20 J cm^{-2}). Non irradiated cells treated with 5 μM PN were used as control, C. Two hours after exposure to light, $\Delta\Psi_m$ was evaluated by flow cytometry using the fluorescent probe JC-1. *P<0.05 compared to control, C; $^{\#}P$<0.05 compared to vehicle. (B, C) The cells were treated as above and harvested 1 h after light exposure. Caspase-8 activity was determined from lysates using the colorimetric tetrapeptidic substrate Ac-IETD-pNA. *P<0.05 compared to control, C; $^{\#}P$<0.05 compared to vehicle, V. Mitochondrial fractions were analyzed by western blot to determine the levels of tBid and COX-IV was used as a loading control. A representative western blot (n=3) is shown.

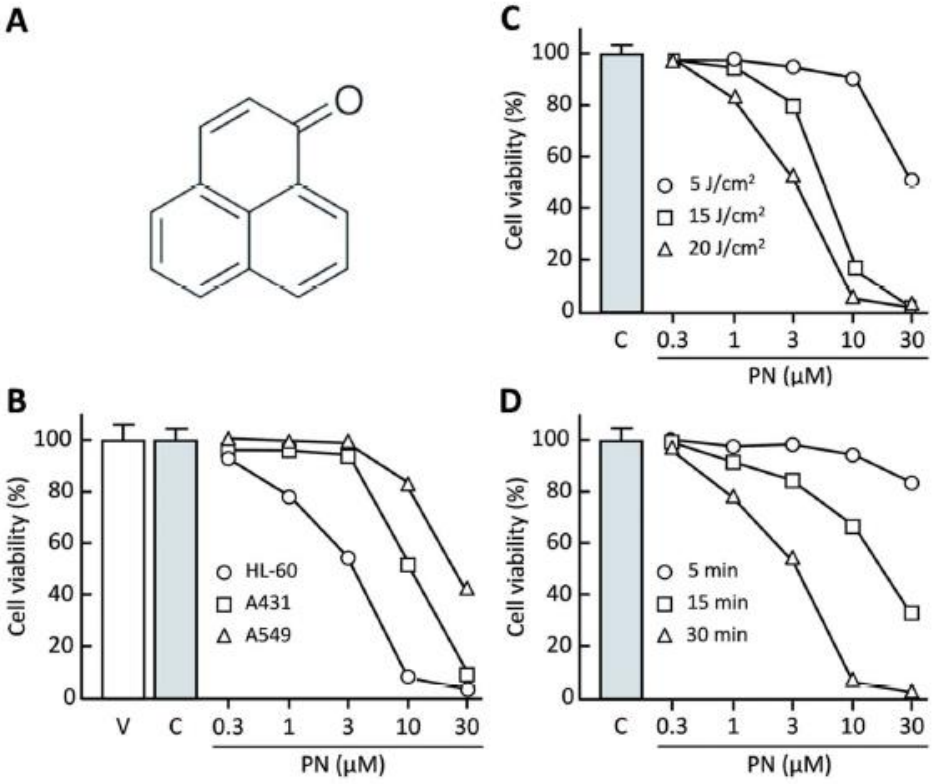

Figure 1

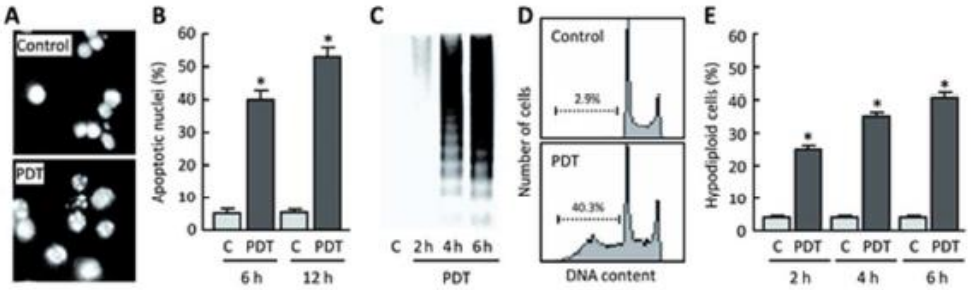

Figure 2

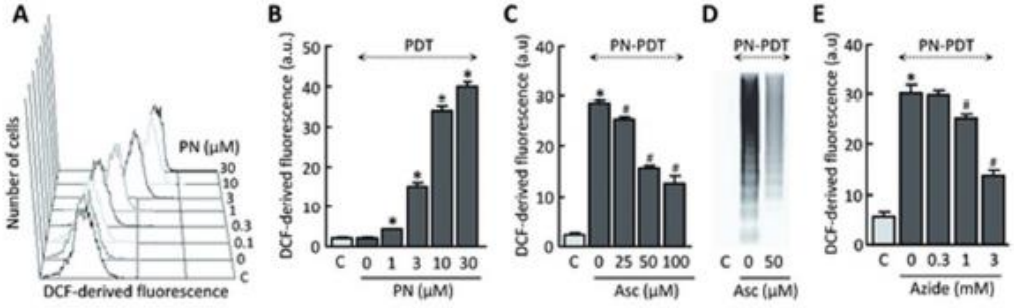

Figure 3

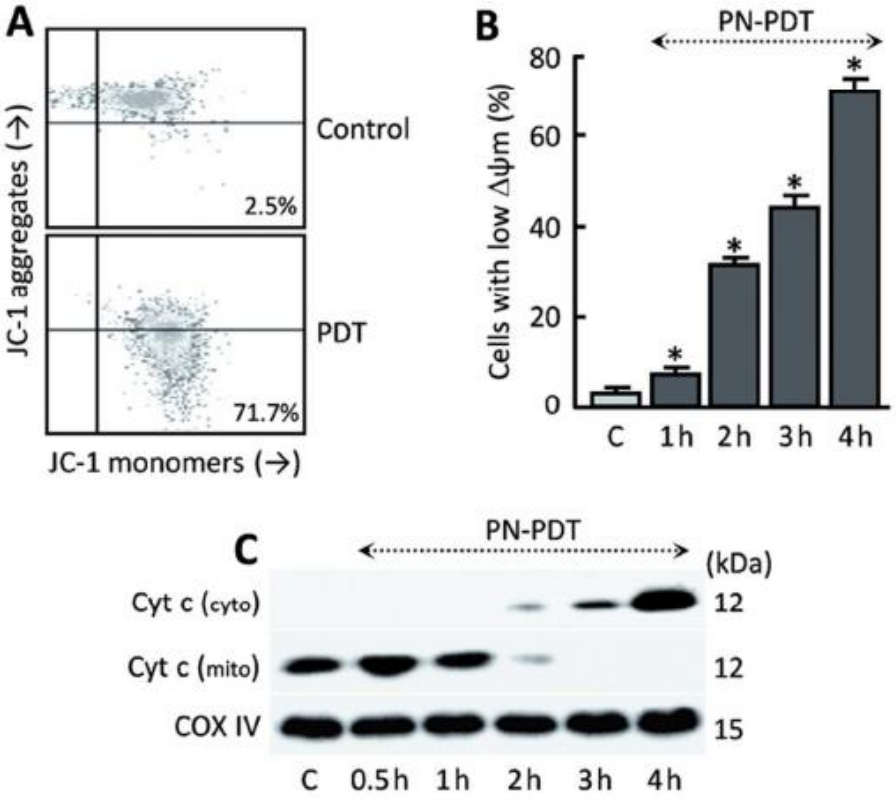

Figure 4

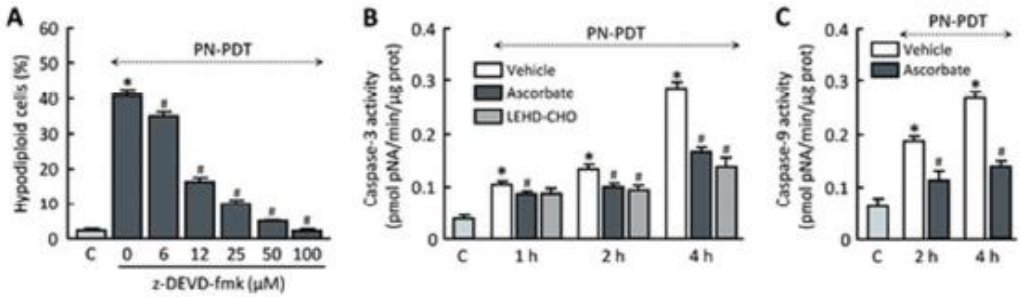

Figure 5

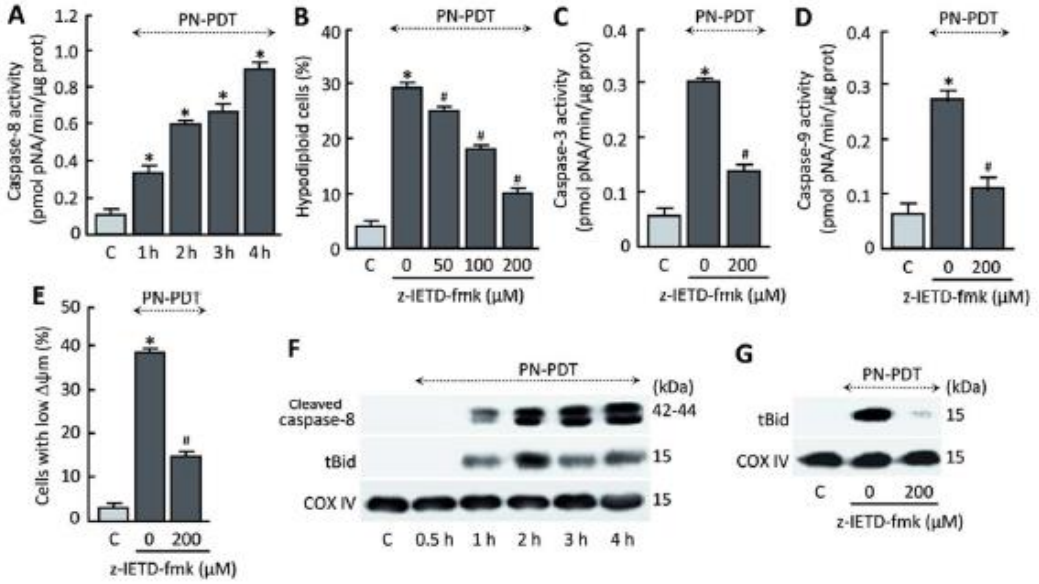

Figure 6

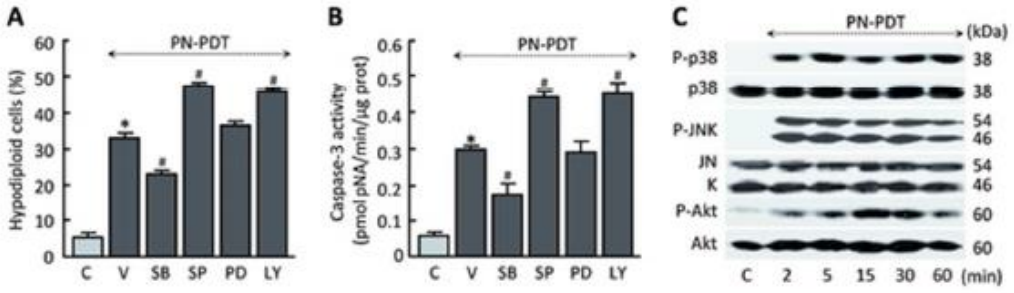

Figure 7

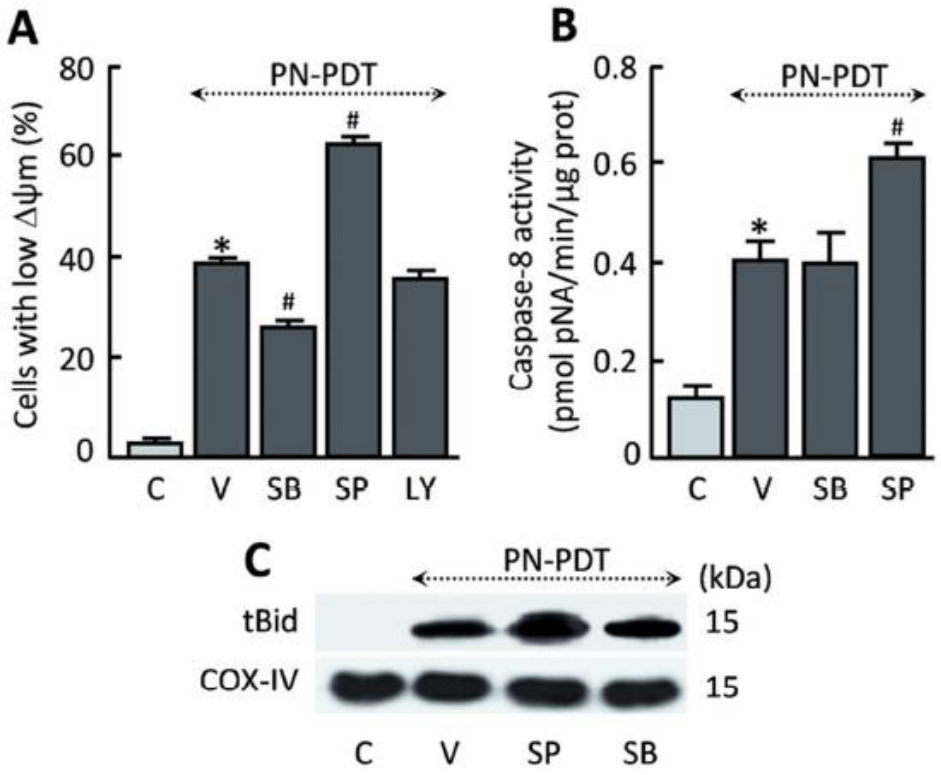

Figure 8